

Numerical study on dehumidifying process in falling film dehumidifier

Sun Jian^{1,2} Shi Mingheng¹

(¹School of Energy and Environment, Southeast University, Nanjing 210096, China)

(²Department of Thermal Energy and Power Engineering, Jingdezhen Ceramic Institute, Jingdezhen 333001, China)

Abstract: A counter flow model of simultaneous heat and mass transfer of a vapor absorption process in a falling film dehumidifier is developed. The governing equations with appropriate boundaries and interfacial conditions describing the dehumidifying process are set up. Calcium chloride is applied as the desiccant. The dehumidifying process between falling liquid desiccant film and process air is analyzed and calculated by the control volume approach. Velocity field, temperature distribution and outlet parameters for both the process air and desiccant solution are obtained. The effects of inlet conditions and vertical wall height on the dehumidification process are also predicted. The results show that the humidity ratio, temperature and mass fraction of salt decrease rapidly at the inlet region but slowly at the outlet region along the vertical wall height. The dehumidification processes can be enhanced by increasing the vertical wall height, desiccant solution flow rates or inlet salt concentration in the desiccant solution, respectively. Similarly, the dehumidification process can be improved by decreasing the inlet humidity ratio or flow rates of the process air. The obtained results can improve the performance of the dehumidifier and provide the theoretical basis for the optimization design, and the operation and modulation of the solar liquid desiccant air-conditioning systems.

Key words: dehumidifier; liquid desiccant; falling film; numerical simulation

Liquid desiccant cooling has a potential use in the air conditioning systems for large buildings because it can reduce electric peak-hour loads during summer time and does not use CFCs which are mainly responsible for ozone layer depletion followed by global warming. The dehumidifier is the most important component of the liquid desiccant cooling system which has been investigated experimentally^[1-2] and numerically^[3-7]. The heat and mass transfer between air and the desiccant solution has also been studied by some investigators. Packed beds are the most popular type in the early systems that are utilized for air dehumidification by liquid desiccants. The performance of packed beds in different configurations and operating conditions using different types of liquid desiccants has been reported^[3-6]. But two major disadvantages, the high pressure drop and the large ratio of desiccant to air mass flow rate, may lead to higher running costs and limit their application^[3,6,8]. In recent years, the falling film dehumidifier has been used extensively in modern process industries and cooling fields, and lots of work has been conducted involving heat and mass transfer because of

its advantages. Especially, its lower air flow rates provide better humidity control and air cooling^[8-9]. However, most of the studies reported in literature on air dehumidification processes use cross^[8] or parallel^[7] flow systems.

This paper focuses on the heat and mass transfer processes between the process air and the desiccant solution in a counter flow dehumidifier. The effects of various operating parameters, and the configurations of the dehumidifier on dehumidification are analyzed. A numerical result for the heat and mass transfer between air and liquid desiccant films in a counter flow dehumidifier during the process of dehumidification of air is given.

1 Mathematical Model of Dehumidification Process

The schematic diagram of air and desiccant solution in the dehumidifier unit is shown in Fig. 1. To simplify the mathematical analysis, the following assumptions are made in the derivation of the steady state governing equations for the proposed dehumidifier: ① The flow in desiccant film is laminar. ② The liquid solution is Newtonian; both liquid and air flows are steady and have constant physical properties. ③ Thermodynamic equilibrium exists at the interface. ④ The

Received 2006-12-07.

Foundation item: The National Natural Science Foundation of China (No. 50276013).

Biographies: Sun Jian (1973—), male, graduate; Shi Mingheng (corresponding author), male, professor, mhshi@seu.edu.cn.

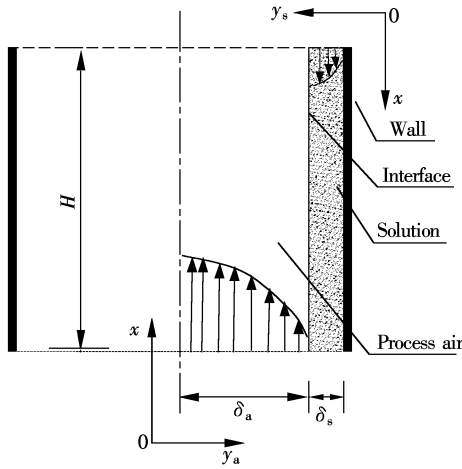


Fig. 1 A schematic diagram of the air and film desiccant flow in a channel

thickness of the film is constant. ⑤ The wall temperature is constant. ⑥ No shear forces are exerted on the liquid by the vapor at the interface. ⑦ Velocity profile is fully developed at the entrance of the channel. ⑧ Body force of air flow is negligible.

1.1 Governing equations for air and desiccant solution

Fig. 1 shows that the desiccant solution flows into the channel from the top of the wall, and the origin of the coordinate is on the top left corner. Based on the preceding assumptions, the equations governing the conservation of momentum, energy and constituents for the desiccant solution can be written as follows.

The momentum equation for the desiccant solution is

$$\nu_s \frac{\partial^2 u_s}{\partial y_s^2} + g = 0 \quad (1)$$

where u_s is the velocity of the desiccant solution in x direction (m/s); g is the gravitational acceleration (m/s²); ν_s is the kinematic viscosity (m²/s).

The energy equation for the two-dimensional heat convection is

$$u_s \frac{\partial T_s}{\partial x} = \alpha_s \frac{\partial^2 T_s}{\partial y_s^2} \quad (2)$$

where T_s is the temperature of the desiccant solution (°C); α_s is the diffusivity of heat in the desiccant solution (m²/s).

The mass conservation equation of water is

$$u_s \frac{\partial \xi}{\partial x} = D_s \frac{\partial^2 \xi}{\partial y_s^2} \quad (3)$$

where ξ is the mass fraction of water in the desiccant solution; D_s is the diffusivity of water (m²/s).

Similarly, the governing equations for the air are

$$\frac{\partial p}{\partial x} = \mu_a \frac{\partial^2 u_a}{\partial y_a^2} \quad (4)$$

$$u_a \frac{\partial T_a}{\partial x} = \alpha_a \frac{\partial^2 T_a}{\partial y_a^2} \quad (5)$$

$$u_a \frac{\partial d}{\partial x} = D_a \frac{\partial^2 d}{\partial y_a^2} \quad (6)$$

where subscript “a” denotes the parameters of process air; d is the humidity ratio of humid air. It should be pointed out that the desiccant solution and process air have a different coordinate system.

1.2 Boundary and interfacial conditions

Based on the flow characteristics of the process air and the desiccant solution as well as the above assumptions, the boundary and interfacial conditions associated with the present problem can be written as

At $x = 0$,

$$T_a = T_{a, \text{in}}, \quad d = d_{\text{in}}, \quad T_s = T_{s, \text{in}}, \quad \xi = \xi_{\text{in}} \quad (7)$$

At $y_a = 0$,

$$\frac{\partial u_a}{\partial y_a} = 0, \quad \frac{\partial T_a}{\partial y_a} = 0, \quad \frac{\partial d}{\partial y_a} = 0 \quad (8)$$

At $y_s = 0$,

$$u_s = 0, \quad \frac{\partial \xi}{\partial y_s} = 0, \quad T_s = T_w \quad (9)$$

At $y_a = \delta_a$,

$$u_a = -u_{s, \text{int}}, \quad d = d^* \quad (10)$$

At $y_s = \delta_s$,

$$\frac{\partial u_s}{\partial y_s} = 0, \quad T_s = T_a \quad (11)$$

$$\left[-k_a \frac{\partial T_a}{\partial y_a} - \rho_a D_a \gamma_{\text{wat}} \frac{\partial d}{\partial y_a} \right]_{y_a = \delta_a} = \left[k_s \frac{\partial T_s}{\partial y_s} \right]_{y_s = \delta_s} \quad (12)$$

$$\left[\rho_s D_s \frac{\partial \xi}{\partial y_s} \right]_{y_s = \delta_s} = \left[-\rho_a D_a \frac{\partial d}{\partial y_a} \right]_{y_a = \delta_a} \quad (13)$$

where subscript “in” denotes inlet parameters; $u_{s, \text{int}}$ is the velocity of the desiccant solution at the interface; T_w is the wall temperature; k is the thermal conductivity (W/(m²·°C)); d^* is the equilibrium moisture content for air at the interface with the desiccant solution and γ_{wat} is the gasification latent heat of water.

1.3 Velocity field in process air

Integrating Eq. (4) and subjected to y_a , we obtain

$$y_a \frac{dp}{dx} = \mu_a \frac{\partial u_a}{\partial y_a} + C_1 \quad (14)$$

Based on the boundary condition (8) and Eq. (14), we can obtain $C_1 = 0$.

Integrating Eq. (14), we obtain

$$\frac{y_a^2 dp}{2 dx} = \mu_a u_a + C_2 \quad (15)$$

Using the boundary condition (10) and Eq. (15), we obtain

$$u_a = -u_{s, \text{int}} - \frac{1}{2\mu_a} \frac{dp}{dx} (\delta_a^2 - y_a^2) \quad (16)$$

Eq. (16) is the velocity equation of process air. Because the mass flux is constant at any cross section, the mass flux m_a of the process air can be written as

$$m_a = \int_0^{\delta_a} \rho_a u_a dy_a \quad (17)$$

where m_a is the mass flow rate of the process air (kg/s). The pressure gradient along the channel is obtained by Eqs. (16) and (17), which can be expressed as

$$\frac{dp}{dx} = -\frac{3\mu_a u_{s,int}}{\delta_a^2} - \frac{3\mu_a m_a}{\rho_a \delta_a^3} \quad (18)$$

Using Eqs. (16) and (18), the velocity profile in the process air is obtained as

$$u_a = -u_{s,int} - \frac{1}{2\mu_a} \left(-\frac{3\mu_a u_{s,int}}{\delta_a^2} - \frac{3\mu_a m_a}{\rho_a \delta_a^3} \right) (\delta_a^2 - y_a^2) \quad (19)$$

1.4 Velocity field in desiccant solution

Integrating Eq. (1), we obtain

$$\nu_s \frac{\partial u_s}{\partial y_s} + g y_s + C_1 = 0 \quad (20)$$

Using the boundary condition (11) and Eq. (20), C_1 can be solved as $g\delta_s$, then integrating Eq. (20) as

$$\nu_s u_s - g\delta_s y_s + g \frac{y_s^2}{2} + C_2 = 0 \quad (21)$$

The velocity in the desiccant solution is obtained by the boundary conditions (9) and Eq. (21) as

$$u_s = \frac{g}{\nu_s} \left(\delta_s y_s - \frac{y_s^2}{2} \right) \quad (22)$$

where δ_s is still unknown.

1.5 Thickness of falling film

The desiccant film thickness can be obtained from the application of the continuity equation at any cross section in the film flow as

$$m_s = \int_0^{\delta_s} \rho_s u_s dy_s \quad (23)$$

where m_s is the mass flow rate of the desiccant solution (kg/s). Using Eqs. (22) and (23), the film thickness can be expressed as

$$\delta_s = \left(\frac{3m_s \nu_s}{\rho_s g} \right)^{\frac{1}{3}} \quad (24)$$

1.6 Equilibrium humidity ratio of process air and desiccant solution

Based on the assumptions, the vapor pressure of the process air should equal the vapor pressure of the desiccant solution at the interface. The equilibrium humidity ratio of air in contact with the desiccant solution is given by the perfect gas relation^[10] as

$$d^* = \frac{0.62185 p_a}{P_{am} - p_a} = \frac{0.62185 p_s}{P_{am} - p_s} \quad (25)$$

where p_s is the vapor pressure of the desiccant solu-

tion; p_a is the vapor pressure of the process air; p_{am} is the total pressure of air.

2 Numerical Method

The discretized representation of this equation is obtained by the control volume method explained in Refs. [8, 11]. The resulting finite difference equations are solved by an iterative method. There are 25 nodes for both process air and desiccant solution in the x -direction, but the coordinate direction is reverse, and in the y -direction there are 100 nodes in the process air side, and 10 nodes in the desiccant side.

3 Results and Analysis

Fig. 2 shows that when the inlet parameters are constant, the humidity ratio of process air and the mass fraction of salt in the desiccant solution decreases along the height of the vertical wall. This is due to the vapor in the process air being absorbed by the desiccant solution.

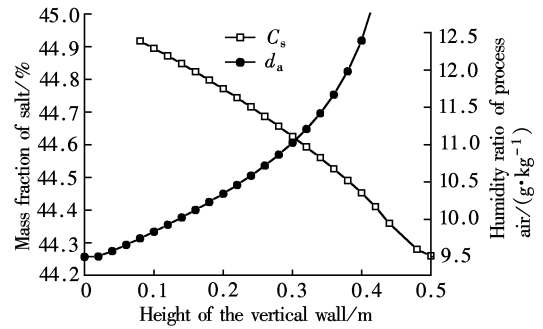


Fig. 2 Variation of C_s and d_a along the wall height at $m_{a,in} = 20.27$ g/s, $m_{s,in} = 50.8$ g/s, $T_{a,in} = 35$ °C, $T_{s,in} = 30$ °C, $C_{s,in} = 45\%$, $d_{a,in} = 20.7$ g/kg

The variations in temperature, the process air and the desiccant solution along the height of vertical wall are shown in Fig. 3. Clearly, the temperature decreases along the channel height, and the temperature decreases rapidly at the inlet region but slowly as height increases since the temperature difference between the film and the wall decreases as channel height increases.

Fig. 4(a) shows the counter-stream humidity ratio distributions in the direction of thickness of the process air in the cases of $H = 0.3$ m, $H = 0.5$ m and $H = 1.0$ m. The humidity ratio decreases in accordance with the thickness of the process air, and the humidity ratio decreases slowly at the symmetry center ($y_a = 0$) but rapidly at the interface since the vapor in the process air transports into the desiccant solution at the interface. At the same time, the dehumidification process is improved as the vertical wall height H increases.

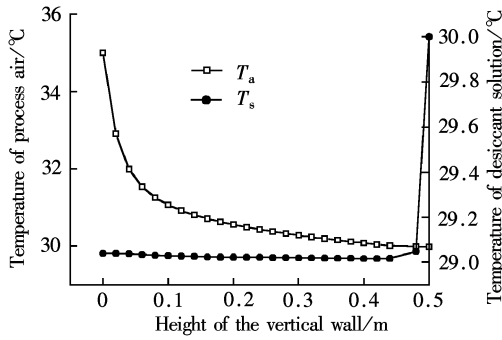


Fig. 3 Variation of T_s and T_a along the wall height at $m_{a,in} = 20.27$ g/s, $m_{s,in} = 50.8$ g/s, $T_{a,in} = 35$ °C, $T_{s,in} = 30$ °C, $C_{s,in} = 45\%$, $d_{a,in} = 20.7$ g/kg

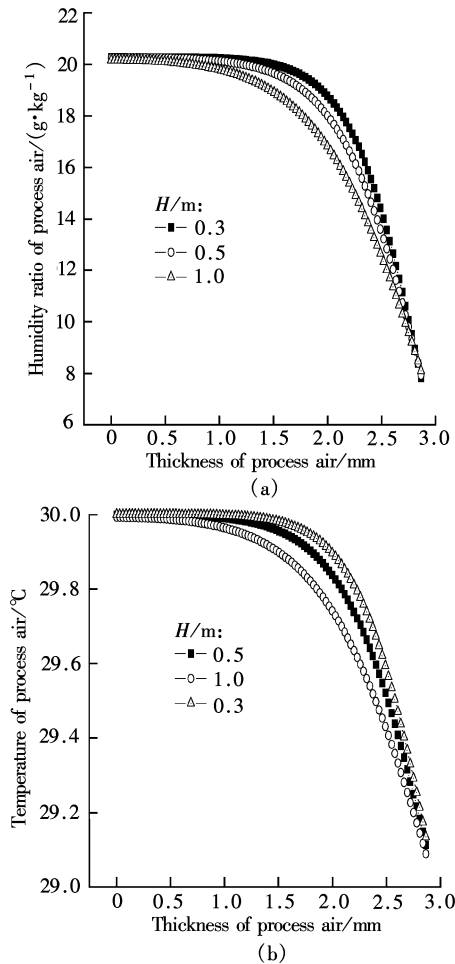


Fig. 4 Variation of d_a and T_a along the thickness of process air for different wall height at $m_{a,in} = 20.27$ g/s, $m_{s,in} = 50.8$ g/s, $C_{s,in} = 45\%$, $d_{a,in} = 20.7$ g/kg

Fig. 4 (b) presents the temperature distribution along the thickness of the process air in the case of vertical wall height $H = 0.3$ m, $H = 0.5$ m and $H = 1.0$ m. The temperature decreases slowly at the symmetry plane ($y_a = 0$) but rapidly at the interface since the temperature difference between the process air and the vertical wall increases as the thickness increases. The temperature distribution is the highest at the symmetry

plane ($y_a = 0$) and decreases to the lowest at the interface since the heat of absorption released at the interface is transported through the liquid film to the plate wall. The dehumidification process is improved as the height of vertical wall H increases.

Fig. 5(a) shows the effect of the inlet temperature of the process air on the humidity ratio along the wall height. Obviously, the inlet temperature of the process air has no effect on the variation in the humidity ratio. Fig. 5(b) presents the effect of the inlet temperature of the desiccant solution on the humidity ratio along the wall height. It is obvious that the inlet temperature of the desiccant solution has a negligible effect on the variation in the humidity ratio.

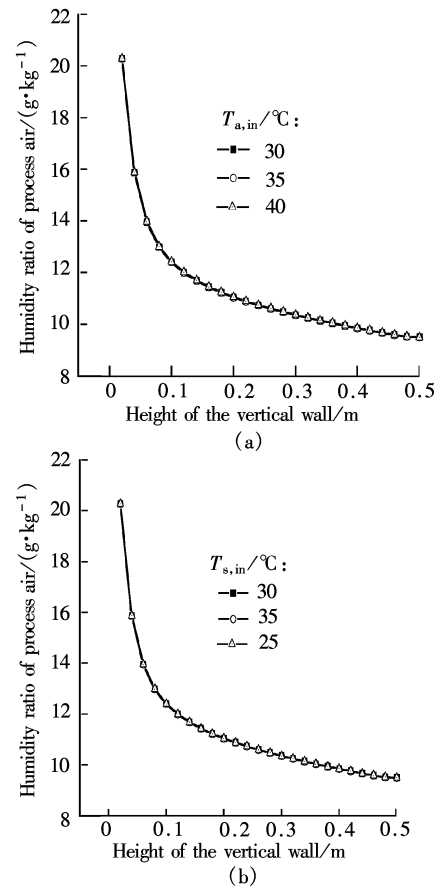


Fig. 5 Variation of d_a along the wall height for different values of T_a and T_s at $m_{a,in} = 20.27$ g/s, $m_{s,in} = 50.8$ g/s, $C_{s,in} = 45\%$, $d_{a,in} = 20.7$ g/kg

The effect of inlet mass flow of the desiccant solution is shown in Fig. 6(a). The outlet humidity ratio decreases rapidly at the desiccant solution inlet region but slowly at the outlet region, and with the increase in the inlet mass flow rate of the desiccant solution the outlet humidity ratio of process air decreases. This is due to the fact that the mass fraction of salt in the desiccant solution decreases along the wall height and the

mass fraction of salt difference is small under high mass fraction of salt and the absorption capacity of solution is high. Fig. 6(b) shows the outlet humidity ratio increases as the process air mass flow rate increases, that is because the mass fraction of salt difference of the desiccant solution decreases along the vertical wall height and the absorption capacity decreases as increase of the mass flow rate of process air.

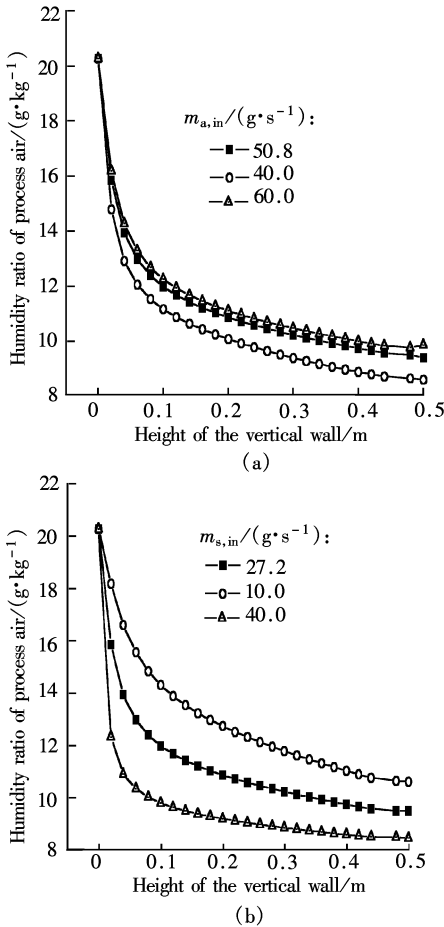


Fig. 6 Variation of d_a along the wall height for different values of $m_{a,in}$ and $m_{s,in}$ at $T_{a,in} = 35^\circ\text{C}$, $T_{s,in} = 30^\circ\text{C}$, $C_{s,in} = 45\%$, $d_{a,in} = 20.7 \text{ g/kg}$

The influence of the inlet mass fraction of salt in the desiccant solution is shown in Fig. 7(a). The inlet mass fraction of salt has an obvious effect on the outlet humidity ratio of the process air along the vertical wall. The dehumidification process is enhanced as anticipated by increasing the inlet mass fraction of salt. It is due to the fact that the mass fraction of salt difference decreases along the wall height and the absorption capacity increases. Then, increasing the mass fraction of salt in the desiccant solution will increase the possibility of crystallization of the salt in the desiccant solution. So, the salt crystallization process limits the highest possible value of the mass fraction of salt in the

desiccant solution. Fig. 7(b) shows that with the increase in the inlet humidity ratio in the process air, the outlet humidity ratio of the process air increases. It is due to the fact that the mass transfer process between air and the desiccant solution increases as the difference between the humidity ratio and the equilibrium humidity ratio increases.

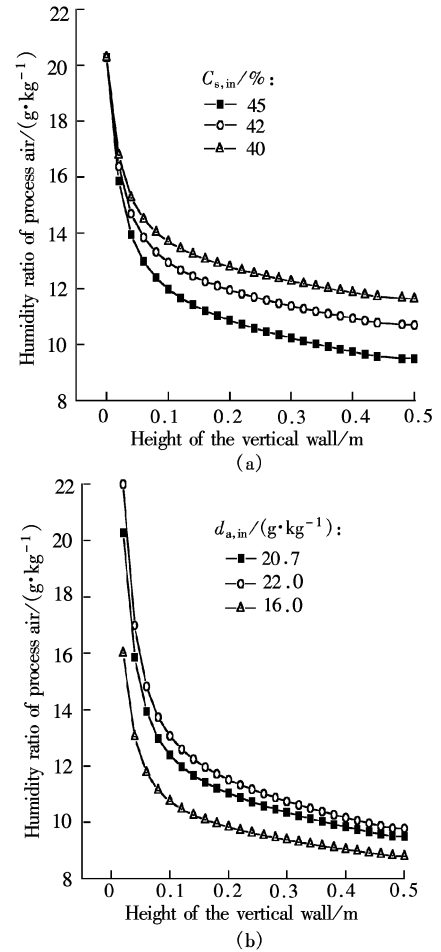


Fig. 7 Variation of d_a along the wall height for different values of $C_{s,in}$ and $d_{a,in}$ at $m_{a,in} = 20.27 \text{ g/s}$, $m_{s,in} = 50.8 \text{ kg/s}$, $T_{a,in} = 35^\circ\text{C}$, $T_{s,in} = 30^\circ\text{C}$, $C_{s,in} = 45\%$, $d_{a,in} = 20.7 \text{ g/kg}$

4 Conclusions

1) The temperature of the process air is at the highest at the symmetry plane of the dehumidifier channel and decreases to the lowest at the interface. Uniform with the temperature profiles, the humidity ratio is the lowest at the interface and increases to the highest at the symmetry plane.

2) The humidity ratio, temperature and mass fraction of salt, both the process air and the desiccant solution, decrease rapidly at the inlet region but slowly at the outlet region depending on the height of vertical wall.

3) The dehumidification process can be enhanced

by increasing the vertical wall height and the desiccant solution flow rates or inlet mass fraction of salt in the desiccant solution, respectively. Similarly, the dehumidification process can be improved by decreasing the inlet humidity ratio or flow rates of the process air.

References

- [1] Patnaik S, Lenz T G, Löf G O G. Performance studied for an experimental solar open-cycle liquid desiccant air dehumidification system [J]. *Solar Energy*, 1990, **44** (3): 123 – 135.
- [2] Pietruschka D, Eicker U, Huber M, et al. Experimental performance analysis and modelling of liquid desiccant cooling systems for air conditioning in residential buildings [J]. *International Journal of Refrigeration*, 2006, **29** (1): 110 – 124.
- [3] Gandhidasan P, Kettleborough C F, Ullah M R. Calculation of heat and mass transfer coefficients in a packed tower operation with a desiccant-air contact system [J]. *Journal of Solar Energy Engineering*, 1986, **108**(2): 123 – 128.
- [4] Gandhidasan P, Ullah M R, Kettleborough C F. Analysis of heat and mass transfer between a desiccant-air system in a packet tower [J]. *Journal of Solar Energy Engineering*, 1987, **109**(2): 89 – 93.
- [5] Radhwan A M, Gari H N, Elsayed M M. Parametric study of a packed bed dehumidifier/regenerator using CaCl₂ liquid desiccant [J]. *Renewable Energy*, 1993, **3**(1): 49 – 60.
- [6] Ren Chengqin, Jiang Yi, Zhang Yianpin. Simplified analysis of coupled heat and mass transfer processes in packed bed liquid desiccant-air contact system [J]. *Solar Energy*, 2006, **80**(1): 121 – 131.
- [7] Stevens D I, Braun J E, Klein S A. An effectiveness model of liquid-desiccant system heat/mass exchanges [J]. *Solar Energy*, 1989, **42**(6): 449 – 455.
- [8] Rahamah A, Elsayed M M, Al-Najem N M. A numerical solution for cooling and dehumidification of air by a falling desiccant film in parallel flow [J]. *Renewable Energy*, 1998, **13**(3): 305 – 322.
- [9] Saman W Y, Alizadeh S. Modelling and performance analysis of a cross-flow type plate heat exchanger for dehumidification/cooling [J]. *Solar Energy*, 2001, **70**(4): 361 – 372.
- [10] ASHRAE Handbook. *Fundamentals* [M]. Society of Heating, Refrigeration and Air-Conditioning Engineers, Inc., 1993.
- [11] Tao Wenquan. *Numerical heat transfer* [M]. 2nd ed. Xi'an: Xi'an Jiaotong University Press, 2004. (in Chinese)

逆流降膜除湿器除湿过程的数值研究

孙 健^{1,2} 施明恒¹

(¹ 东南大学能源与环境学院, 南京 210096)

(² 景德镇陶瓷学院热能与动力工程系, 景德镇 333001)

摘要:建立了模拟逆流降膜除湿过程传热传质的数学模型,给出了传热传质的控制方程和适当的边界条件和气液界面条件.采用氯化钙作为除湿剂,运用控制容积法对降膜除湿溶液与被处理空气之间的除湿过程进行了分析和计算.获得了相应的除湿溶液与被处理空气的速度场、温度分布和出口参数.计算结果表明:沿着除湿器高度方向溶液和空气的温度、溶液的浓度、空气的湿度在入口区域变化较快而在出口区域变化较慢.可分别通过增加竖壁的高度、溶液的入口浓度和溶液的流速来改善除湿过程;同样,也可通过降低空气的流速或空气入口湿度达到改善除湿过程的目的.研究结果有利于改进除湿器的性能,为太阳能液体除湿、空调系统的优化设计和运行调节提供了理论依据.

关键词:除湿器;液体除湿剂;降膜;数值模拟

中图分类号:TQ021